JOURNAL OF OPTOELECTRONICS AND ADVANCED MATERIALS Vol. 12, No. 12, December 2010, p. 2400 - 2405

Electrical characteristics and photoresponse of n-ZnSe/p-GaP heterojunction prepared by metal organic chemical vapor deposition

M. FADEL, A. A. M. FARAG[a*]
Semiconductor lab.,Physics department,faculty of Education,Ain Shams University, Egypt
[a]Thin Film Lab., Physics department,faculty of Education,Ain Shams University, Egypt

In this paper, the n-type ZnSe films were grown on p-type GaP single crystalline substrate by metal organic chemical vapor deposition ,MOCVD. The temperature dependence of current–voltage (*I–V*) characteristics of n-ZnSe/p-GaP heterojunction contacts were measured in the temperature range 300-425 K. These characteristics show rectifying behaviour consistent with a potential barrier formed at the interface. The high values of ideality factor (*n*) may be ascribed to the presence of an interfacial layer .The density of interface states N_{ss} distribution profile as a function of (E_{ss}-E_v) was extracted from the forward bias I-V measurements . The photovoltaic parameters such as open circuit voltage and short circuit current were studied as a function of incident light intensity. The photoresponse measurements showed a logarithmic variation of open circuit voltage with the incident light intensity and show an improvement of the ideality factor under effect of illumination.

(Received October 28, 2010; accepted November 25, 2010)

Keywords: n-ZnSe/p-GaP;MOCVD, Photoresponse

1. Introduction

ZnSe is an important semiconductor material with cubic zinc blende structure and with a direct band-gap of 2.7 eV, is found to be a very promising material for optoelectronic and heterojunction solar cells. It has been used in many applications such as a protective and antireflection coating for infrared-operating electrochromic thermal-control surfaces [1], light-emitting diodes [2–3], dielectric mirrors [4] and photodiodes [5,6]. Since most electronic devices are produced in the form of thin film, for any such applications, the material preparation and characterization plays a vital role and also the crystal- lographic quality of thin films largely depends on the ambient pressure and lattice match [7]. The growth and study of the prepared film on lattice-matching substrates also plays a crucial role for such applications. The structures are usually grown on III-V substrates due to the lack of appropriate II-VI bulk crystals. However, this causes problems related to the II-VI / III-V interface[8] . Epitaxial overgrowth is well established for the common semiconductor materials such as silicon, GaAs, GaP, and InP [9-12]. Hybrid systems based on these different classes of materials reveal interesting electronic and optical properties [13].The growth of the single-crystal layers of ZnSe have been grown on GaP and GaAs substrates in a hydrogen transport system by Fuke et al .[14] . They found that the growth on GaP (111) substrates was limited by thermodynamic mass transport and that on GaP (100) substrates by the kinetics of the surface chemical reaction. They also noticed that ZnSe layers grown on the GaAs (100) face have larger growth rates and smoother surface morphologies than those on GaP (100). This result may originate from the lattice parameter mismatch between the epitaxial layers and the substrates.The interface states of heterojunction or Schottky diode structures play an important role for the understanding of the electrical properties of these structures[15,16] . Some parameters which are such as ideality factor, barrier height, and series resistance influence the performance of the device. These parameters give useful information concerned with the nature of the diode. The classical model of Schottky diode assumes the junction to be abrupt with a fixed barrier height. To understanding the barrier formation at metal–semiconductor interfaces on a fundamental basis still remains a challenging problem[17,18]. In addition, it is necessary to determine the diode parameters over a wide range of temperature at heterojunction or metal/semiconductor interface to understand the nature of barrier and conduction mechanism. Because, analysis of *I–V* characteristics of these contacts measured only at room temperature does not give detailed information about its conduction process and interface characteristics. In this study, A thin ZnSe films were grown on single crystalline GaP by MOCVD processes for the preparation of the ZnSe/GaP heterojunction structures, and temperature dependences of the ideality factors, barrier heights and interface state densities of these structures have been analysed in a wide temperature range. The *I–V and C-V*

measurements of the heterojunctions have been carried out under laboratory conditions in dark, and at temperatures ranging from 300 to 425K .

2. Experimental details

ZnSe epitaxial layers were grown on p-type GaP (100) substrates using a Metal Organic Chemical Vapor Deposition, MOCVD, system with a horizontal reactor founded in University of Manchester Institute of Science and Technology UMIST, UK.

Diethylzinc (DEZn) was used as the source for Zn, selenium hydride (H_2Se) was used as the source Se. H_2 was used as the gas carrying the sources , and the total flow rate was kept at 2.3 litre/s.

Just prior to growth , the wet etched GaP substrates were deoxidized at 620 ^oC under tertiary butyl phosphine . Homoepitaxial buffers were grown using tri-methyle-gallium . Epitaxy of the ZnSe layers was started after cooling the substrates to 350 ^oC under group V ambient , and a subsequent purge of 10 s duration without group V stabilization .

For the I–V measurements, stabilized power supply and high-impedance keithley 617 electrometer were used. The dark C–V measurements were performed at different temperatures using a computerized high frequency (1MHz) capacitance–voltage system consisting of C–V meter (model 4108, Solid State Measurement, Inc., Pittsburg). The temperature of samples was measured during electrical measurements by NiCr–NiAl thermocouple with accuracy ±1 K. The high power halogen lamp containing iodine vapor and tungsten filament was used for the illumination of the device. The intensity of light was measured with a solar power meter (BTU- Solar Power Meter TM-206, Taiwan). The intensity of light was varied by changing the distance between the device and the halogen lamp. The intensity of light was varied by changing the voltage across the lamp.

3. Results and discussion

3.1 Dark I-V characteristics

The electrical characterizations of the n-ZnSe/p-GaP device were achieved through current–voltage measurements in the temperature range of 300–425K under forward and reverse bias are shown in Fig.1 . It is observed from this figure that the junction exhibits strong rectifying characteristics showing a n-p diode –like behavior . The rectification ratio,RR was recorded for the all temperature range and tabulated in Table 1 .It is observed from this table that the rectification ratio, RR ratio has decreased with increasing temperature and then the best rectification ratio can be obtained at room temperature (300K) for n-ZnSe/p-GaP heterojunction.

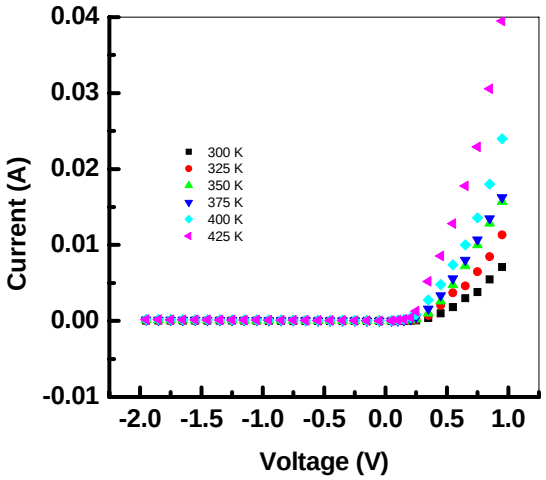

Fig. 1 Current–voltage characteristics of the n-ZnSe/p-GaP heterojunction at different temperature.

Table 1 current-voltage parameters of n-ZnSe/p-GaP heterojunction

T(K)	RR	n	Φ_{bo}(eV)	High voltage range		δ(μm)
				$R_s(\Omega)$	n	
300	260	2.67	0.67	38.3	4.9	0.067
325	204.5	2.29	0.72	30	3.8	0.0236
350	195	1.89	0.78	25.7	2.76	0.0216
375	169.5	1.67	0.82	20.4	2.04	0.0198
400	161	1.62	0.85	16.2	1.79	0.0186
425	271	1.52	0.89	12.2	1.38	0.0175

Current–voltage (*I–V*) measurements are one of the methods to determine some electrical properties in diodes. The forward bias *I–V* characteristics of the n-ZnSe/p-GaP structure at different temperatures are given in Fig. 2. Firstly, let us discus the temperature-dependent data according to thermionic emission current model. The current –voltage through a uniform interface due to thermionic emission can be expressed as [19,20]

$$I = I_0 \exp\left(\frac{qV}{nkT}\right)\left[1-\exp\left(-\frac{qV}{kT}\right)\right] \qquad (1)$$

where I_o is the reverse saturation current and described by

$$I_0 = AA^*T^2 \exp\left(-\frac{q\Phi_{b0}}{kT}\right) \qquad (2)$$

where A is the diode area, k the Boltzmann constant, n is the ideality factor, A* the effective Richardson constant of holes in p-type GaP was calculated as A*=120 m_e^*/m_0=92.5 A/(cm^2 K^2) [21] , Φ_{b0} the effective barrier height at zero bias and T is the absolute temperature. The forward bias I–V characteristics of the n-ZnSe/p-GaP heterojunction structure at room temperature are shown in Fig. 2.

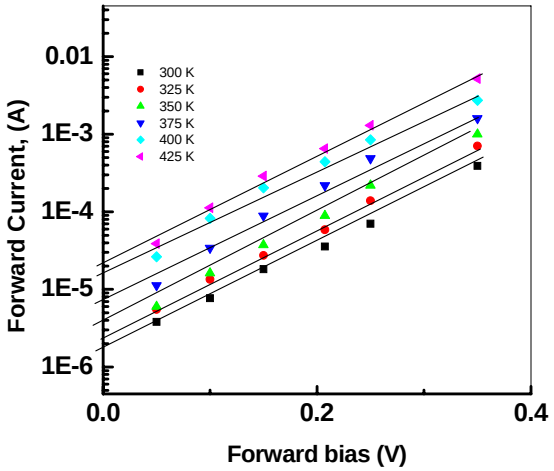

Fig.2 Plots of the forward I–V of the n-ZnSe/p-GaP heterojunction at different temperatures.

The ideality factor ,n was introduced to take into account the deviation of the experimental I-V data from the ideal thermionic model and therefore it can be calculated from the fit equation from a plot of natural log of current versus forward bias voltage in the range approximately between 0 and 0.4 V(Fig.2) . Fig.2 shows a straight lines and then the effect of series resistance in this voltage region is small and can be neglected in this voltage range . The experimental values of n in the temperature range 300-425 for n-ZnSe/p-GaP heterojunction are listed in Table 1 . As observed, our sample with large value of n is far from the ideal case due to the presence of a thick interfacial oxide layer and the interface states. The non-linearity of I–V characteristics at high bias values(see Fig.1) indicated a continuum of interface states, which equilibrate with semiconductor . This suggests that the effect of series resistance on the ZnSe/GaP heterojunction cannot be ignored at this region [22,23]. Therefore, the series resistance can be obtained using the following equation [24]

$$\frac{dV}{d\ln(I)} = n\frac{kT}{q} + IR_s \qquad (3)$$

The plots of dV/dln I vesus I are shown in Fig. 3 . The series resistance and ideality factor were determined from the slope and intercept of the fit linear shown in Fig.3 . The obtained values are given in Table 1. As illustrated, the obtained high values of series resistance for the investigated junction can be due to due to the presence of interfacial layer and to the high resistance of the starting semiconductors.

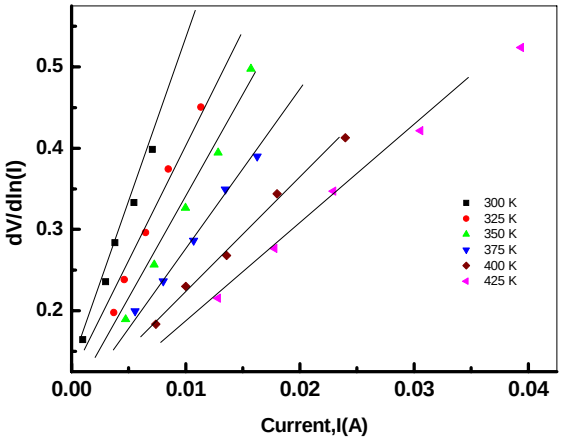

Fig. 3. Plots dV/dlnI vs. I of the n-ZnSe/p-GaAs heterojunction at different temperatures.

The most important characteristic of the n-ZnSe/p-GaP interface is the nature of the potential barrier between the Fermi level and the majority carriers band edge of the semiconductor at the ZnSe/GaP interface [23] . This potential barrier is of central importance for determining the performance of the semiconductor devices, since electrical contacts to semiconductors necessitate interfaces and depending upon the barrier height. Such interfaces will exhibit a modest resistance to current flow in either direction over a large temperature range or a low resistance to flow current in one direction and high resistance to current flow in the opposite direction [25].

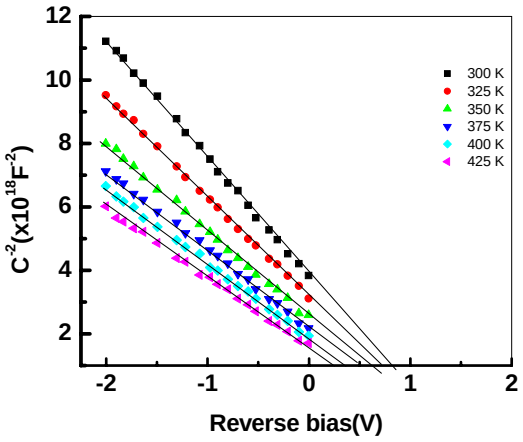

Fig.4 Plots of $1/C^2$ vs. V of the n-ZnSe/p-GaAs heterojunction at different temperatures.

The experimental values of the zero-bias barrier height ,Φ_{b0} were determined using the values of reverse saturation current derived from the straight line intercept of the natural log current axis at zero bias (V=0) (Fig.2) and Eq.(2) . The experimental values of Φ_{b0} are given in Table (1). As observed, the values of Φ_{b0} increase with increasing temperature in the considered temperature range. When the temperature increases, more and more electrons have sufficient energy to surmount the higher barrier .As a result , the dominant barrier height will increase with the temperature and voltage [26]

The voltage dependence of the effective barrier height Φ_e due to the interfacial layer is given as [27].

$$\Phi_e = \Phi_{b0} + \beta\left(V - IR_s\right) = \Phi_{b0} + \left(1 - \frac{1}{n(V)}\right)\left(V - IR_s\right) \quad (4)$$

by considering the applied voltage dependence of the barrier height, where β is the voltage coefficient of the effective barrier height Φe which used instead of barrier height Φ_{b0} . Φ_e is considered as a parameter that combines the effects of both interface states equilibrium with the semiconductor [28, 29].

The density of the interface states of the n-ZnSe/p-GaP heterojunction structure can be obtained from the forward bias I–V characteristics at each temperature by the following relation [30]:

$$N_{ss}(V) = \frac{1}{q}\left[\frac{\varepsilon_i}{\delta}\left(n(V) - 1\right) - \frac{\varepsilon_s}{W_D}\right] \quad (5)$$

where W_D is the space charge width, δ is the thickness of interfacial insulator layer, N_{ss} is the density of interface states; ε_s (11.1ε_0) and ε_i (3.8ε_0) are the permittivity of the semiconductor and interfacial layer, respectively[31]. Furthermore, in p-type semiconductor, the energy of the interface states, E_{ss} with respect to the bottom of the valance band E_V at the surface of the semiconductor is given by [31-33]:

$$E_{ss} + E_V = q\left(\Phi_e - V\right) \quad (6)$$

where E_{ss} is the energy corresponding to the top of the valance band at the surface of semiconductor .

3.2 Dark C-V characteristics

C–V analysis was done at 1 MHz as a function of reverse bias in the temperature range 300-425 K . Fig. 4 shows $1/C^2$–*V* characteristics of a typical n-ZnSe/p-GaP heterojunction. The intercept of $1/C^2$–*V* gives (by extrapolating the straight line to the *X*-axis) is essentially equal to the diffusion potential within the GaP. Considering the junction as abrupt junction, $1/C^2$ vs. *V* can then be expressed as [17]. The carrier concentration can be determined from the following relation

$$\frac{A^2}{C^2} = \frac{2\left(V_b - V - \left(kT/q\right)\right)}{q\varepsilon_s N_A} \quad (7)$$

where ε_s is the permittivity of GaP, N_A is effective carrier concentration, *A* the junction area, *V* the applied voltage, and V_b the built-in potential. This plot reveals a good linear nature indicating that the abrupt heterojunction theory is indeed applicable to the n-ZnSe/p-GaP structure. The slope of the plot gives $N_A = 9.97 \times 10^{16}$ cm^{-3} which is consistent with the resistivity of the p-GaP [29]. For a device of an area 0.18 cm^2 the depletion width *W* calculated from Eq. (4) is found to be 65.1 nm.

The depletion width of the junction is given by the relation

$$W = \sqrt{\frac{\varepsilon_s \varepsilon_0 \left(V_b - V\right)}{q N_A}} \quad (8)$$

where ε_s is the dielectric constant (ε_s = 11.1) [30] of GaP and ε_0 is the vacuum permittivity. The C^{-2} versus applied voltage for the investigated junction is shown in Fig. 4. Before n-ZnSe and p-GaP are in contact, n-ZnSe has high concentration of electrons and few holes compared to that of p-GaP. Upon contacting, diffusion of carriers will take place at concentration gradient at the junction. The electrons will diffuse from n-ZnSe to p-GaP and negative space charge will remain behind in p-GaP near the junction. At zero voltage bias due to diffusion of holes in n- ZnSe from p-GaP valence band energy increases hence band bends downwards in p-GaP. But in p-GaP due to diffusion of holes valence band energy decreases thus band bends upward. As the hole concentration is more in nitrogen doped ZnSe compared to that of p-GaP band bends more towards GaP.

The interfacial insulator layer thickness δ was obtained from high frequency (1 MHz) C–V characteristics(Fig.5) using the equation for insulator layer capacitance ($C_{ox} = \varepsilon_i \varepsilon_o$ A/δ), where $\varepsilon_i = 3.8\,\varepsilon_o$ [34,35]. The values of δ were calculated in the temperature range 300-425 K and given in Table 1.

The density of the interface states as a function of (E_{ss}-E_v) is shown in Fig. 5. It is seen an exponential decrease in the values of N_{SS} when the (E_{ss}-E_V) increases. The increase in N_{ss} values after reaching a minimum value originates from the mid gap towards the bottom of the valence band in GaP . This increase is probably due to the increase in the series resistance[36].

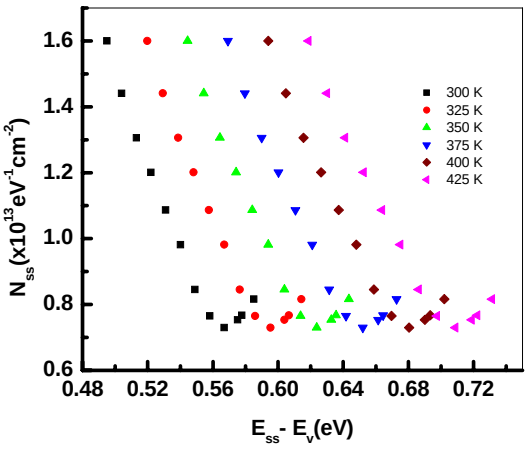

Fig.5 Plots of N_{ss} vs. E_{ss}-E_v of the n-ZnSe/p-GaAs heterojunction at different temperatures.

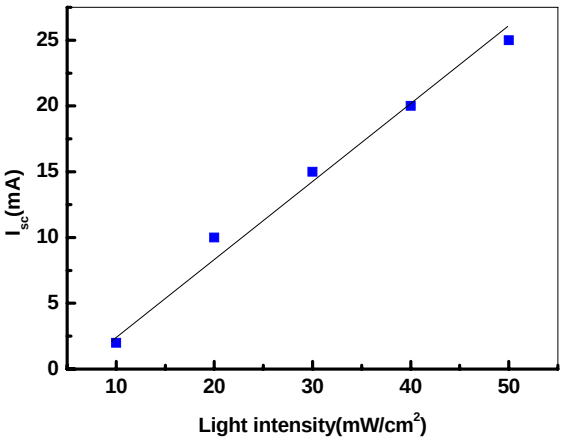

Fig. 6 Plots of I_{sc} vs. light intensity of the n-ZnSe/p-GaAs heterojunction

The temperature dependence of the N_{ss} is also shown in Fig. 5. It is show that the values of N_{ss} increase with decreasing temperature.

3.3 Photoresponse characterization

To study, the response of the n-ZnSe/p-GaP heterojunction towards light, the cell was illuminated with light of different intensity. The open circuit voltage and short circuit current were measured as function of light intensity. Fig. 6 shows variation of short circuit current (I_{sc}) as a function of light intensity, whereas, Fig. 7 shows the variation of open circuit voltage as a function of light intensity. The photoresponse measurements showed a logarithmic variation of open circuit voltage with the incident light intensity. However, at higher intensities, saturation in open circuit voltage was observed, which can be attributed to the saturation of the electrolyte interface, charge transfer and non-equilibrium distribution of electrons and holes in the space charge region of the photoelectrode. But short circuit current follows almost a straight-line path. The photoelectrode–electrolyte interface can be modeled as a Schottky barrier solar cell and it is therefore possible to represent the current–voltage relationship as

$$I = I_{ph} - I_d = I_{ph} - \left[I_0 \exp\left(\frac{qV}{nkT}\right) - 1 \right] \qquad (9)$$

where I is the net current density, I_{ph} is the photocurrent densities, I_d is the dark current density, I_0 is the reverse saturation current density, V is the applied bias voltage. In bias voltage condition $V > 3kT/q$ and at equilibrium open circuit conditions;

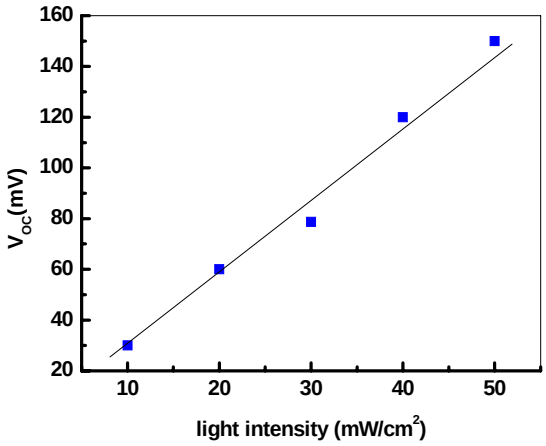

Fig.7 Plots of V_{oc} vs. light intensity of the n-ZnSe/p-GaAs heterojunction

$I_{ph}=I_d$ and $V=V_{oc}$

Thus,

$$V_{oc} = \left(\frac{n_L kT}{q}\right) \ln\left(\frac{I_{sc}}{I_0}\right) \qquad (10)$$

where V_{oc} is open circuit voltage, I_{sc} is short circuit current. As $I_{sc} \gg I_0$, a plot of log I_{sc} against V_{oc} should give a straight line and from the slope of the line the lighted ideality factor can be determined. The plot V_{oc} versus I_{sc} for n-ZnSe/p-GaP photoelectrode is shown in Fig. 8. The lighted ideality factor was calculated and found to be 1.5 which give evidence for the improvement of the performance of the n-ZnSe/p-GaP heterjunction under illumination.

4. Conclusion

In conclusion, the effect of density of interface states and series resistance in n-ZnSe/p-GaP structures has been characterized and analyzed. It was fount that the value of n calculated from forward bias I–V measurement was greater than unity. This behaviour can be ascribed to the interfacial layer and interface states. The applied bias voltage drops partially across the interfacial layer causing the forward current to drop, thus producing a strong deviation from the ideal I–V characteristics. Temperature dependence of the energy distribution of the interface states density profile could be determined from the forward bias I-V and C-V characteristics. The various performance parameters were determined for the investigated junction as a photodiode .

Acknowledgment

The authors would like to acknowledge Dr.A.A.Nijim, Physics Department, Al-Azhar University,Gazza, Gazza Strip , for kindly supplying the n-ZnSe/p-GaP devices .

References

[1] L. Yan, J.A. Woollam, E. Franke, J. Vac. Sci. Technol. A **20**(3), 693 (2002).
[2] T. Shi rakawa, Mater. Sci. Eng. B **91**(92) 470 (2002).
[3] M. Godlewski, E. Guziewicz, K. Kooalko, E. Lusakowska, E. Dynowska, M. M. Godlewski, E. M. Godys, M.R. Phillips, J. Lumin. **102–103**, 455 (2003).
[4] H.R. Dobler, Appl. Opt. **28**, 2698 (1989).
[5] W. S. Lour, C.-C. Chang, Solid State Electron. **39**, 1295 (1996).
[6] B. Ullrich, Mater. Sci. Eng. B **56,** 69 (1998).
[7] R. F. C. Farrow, G. R. Jones, G. H. Williams, I. M. Young, Appl. Phys.Lett. **39**, 954 (1981).
[8] C. Meynea, M. Genscha, S. Petersb, U.W. Pohla, J. T. Zettlera, W. Richter Thin Solid Films **364**, 12 (2000).
[9] R. Bergmann, E. Bauser, J. H. Werner, Appl. Phys. Lett. **57**(4), 351 (1990).
[10] G. W. Neudeck, P. J. Shubert, J. L. Glenn, J. A. Friedrich, W.A. Klaasen, R.P. Zingg, J. P. Denton, J. Electron.Mater. **19** (10), 1111 (1990).
[11] B.-Y. Tsaur, R.W. McClelland, J.C.C. Fan, R.P. Gale, J. P. Salerno, B. A. Vojak, C. O. Bozler, Appl. Phys. Lett. **41**(1) 347 (1982).
[12] S. Zhang, T. Nishinaga, J. Crystal Growth **99**, L2427 (1990).
[13] B. Roy, S. Roy, D. Chakravorty, J. Mater. Res. **9**, 2677 (1994).
[14] S. Fuke, K. Ogawa, K. Kuwahara, T. Imai, J. Appl. Phys. **61,** 4920 (1987)
[15] A. Türüt, F. Kleli, J. Appl. Phys. **72**, 818 (1992).
[16] Z. Hai-feng., W. Chong-yu, F. Rong-chuan. B.Da-yan, LI Yong. CHIN.PHY S.LETT. **14**, 128 (1997).
[17] A. Frey, FLehmann, P. Grabs,C. Gould, GSchmidt, K. Brunnerand, L. W. Molenkamp Semicond.Sci.Technol. **24**, 035005 (2009).
[18] C. Coskun, M. Biber, H. Efeoglu, Appl. Surf. Sci. **211**, 363 (2003).
[19] E. H. Rhoderick, R.H. Williams, Metal Semiconductor Contacts (second ed.), Clarendon Press, Oxford (1988).
[20] S.M. Sze, Physics Semiconductor Devices, New York, 1981.
[21] Meyer, L.R. Ram-Mohan, Jorunal of Applied Physics, **89**, 5815 (2001)
[22] K. Akkilic,I.Uzun,T.Kilicoglu,Synth.Met. **157**, 297 (2007).
[23] T.Kilicoglu,ThinSolid Films **516**, 967 (2008).
[24] Ş. Altındal, S. Karadeniz, N. Tuğluoğlu, A. Tataroğlu, Solid State Electron. **47**, 1847 (2003).
[25] M. E. Aydin, F. Yakuphanoglu,J.Phys.Chem.Solids **68**, 1770 (2007)
[26] C.Coskun ,M.Biber,H.Efeoglu, ,J.Appl.Surf.Sci., **211**, 363 (2003).
[27] H.C.Card ,E.H.Rhoderick ,J.Phys.D **4**, 1589 (1971).
[28] P. Chattopadhyay, A. N. Daw, Solid State Electron. **29**, 555 (1986).
[29] H. A. Çetinkara, A. Türüt, D.M. Zengin, Ş. Erel, Appl. Surf. Sci. **207**, 190 (2003).
[30] H.C. Card, E.H. Rhoderick, J. Phys. D **4**, 1589 (1971).
[31] S. Zeyrek, S. Altındal, H. Yüzer, M.M. Bülbül, Appl. Surf. Sci. **252**, 2999 (2006)
[32] S. Karatas, S . Altındal, M. C¸ akar, Physica B **357**, 386 (2005).
[33] M. Saglam, E. Ayyildiz, A. Gümüs, A. Türüt, H. Efeo˘glu, S. Tüzemen, Appl. Phys.A **62**, 269 (1996).
[34] Ş. Altındal, S. Karadeniz, N. Tuğluoğlu, A. Tataroğlu, Solid State Electron. **47**, 1847 (2003).
[35] S.M. Sze, Physics Semiconductor Devices, second ed., New York, 2002.
[36] F. Yakuphanoglua, Burm-Jong Leeb Physica B **390**, 151 (2007).

*Corresponding author: alaafaragg@yahoo.com.